Journal of Molecular Liquids 417 (2025) 126671

Contents lists available at ScienceDirect

Journal of Molecular Liquids

journal homepage: www.elsevier.com/locate/molliq

Acid-base properties of hydroxyquinolines in aqueous solution: Effect of hydroxyl group position on thermodynamic protonation parameters

Anna Baryłka [a], Giuseppina D.G. Santonoceta [b], Giuseppe Gattuso [c], Beata Godlewska-Żyłkiewicz [d], Carmelo Sgarlata [b,*], Demetrio Milea [c,*], Sofia Gama [d,e,**]

[a] University of Bialystok, Doctoral School of Exact and Natural Sciences, K. Ciołkowskiego 1K, 15-245 Bialystok, Poland
[b] Dipartimento di Scienze Chimiche, Università degli Studi di Catania, Viale Andrea Doria 6, 95125 Catania, Italy
[c] Dipartimento di Scienze Chimiche, Biologiche, Farmaceutiche ed Ambientali, CHIBIOFARAM, Università degli Studi di Messina, Viale F. Stagno d'Alcontres 31, 98166 Messina, Italy
[d] Department of Analytical and Inorganic Chemistry, Faculty of Chemistry, University of Bialystok, K. Ciołkowskiego 1K, 15-245 Białystok, Poland
[e] Centro de Ciências e Tecnologias Nucleares, Instituto Superior Técnico, Universidade de Lisboa, Estrada Nacional 10 (km 139.7), 2695-066 Bobadela LRS, Portugal

ARTICLE INFO

Keywords:
Hydroxyquinolines
Thermodynamic parameters
pH potentiometry
Isothermal titration calorimetry
UV–Vis spectrophotometry

ABSTRACT

The acid-base properties of 2-hydroxyquinoline (2-HQ), 4-hydroxyquinoline (4-HQ), 6-hydroxyquinoline (6-HQ), and 8-hydroxyquinoline (8-HQ) were investigated in this work by UV–Vis spectrophotometry, ISE-H^+ potentiometry (glass electrode) and Isothermal Titration Calorimetry (ITC) in $KCl_{(aq)}$ at $I = 0.2$ mol·dm^{-3}, and $T = 298.15$ K. Potentiometric titrations were also performed at different temperatures ($288.15 \leq T/K \leq 318.15$) to derive, together with direct ITC measurements, the corresponding protonation enthalpy and entropy changes. The analysis of the results obtained using various techniques allowed for a comprehensive characterization of the thermodynamic profile and chemical speciation of the studied hydroxyquinolines. Most importantly, it enabled the evaluation of how the position of the hydroxyl group influences the stability and driving forces involved in the protonation/deprotonation processes of both the quinolinic nitrogen and the hydroxyl groups on the pyridine or benzene ring of the hydroxyquinolines.

1. Introduction

Quinolines gathered considerable attention and importance in various branches of medicine and chemistry, mainly due to their therapeutic potential. Due to its manifold properties, quinolinic ring has become a "parental" skeleton for the synthesis of new medicinally valuable derivatives. Extensive data from the literature show how the quinoline structure allows the addition of many functional substituents in various ring positions, favoring the synthesis of many derivatives [1–5]. Furthermore, many pharmacologically relevant natural products contain quinoline as a substructure, displaying a broad spectrum of drug scaffolds [5,6], being reported several quinoline derivatives exhibiting a broad range of biological activities, as anti-inflammatory, antimalarial and antimicrobial effects, revealing their potential as therapeutic agents in the treatment of several diseases, from cancer to neurodegenerative disorders [7–9]. Among quinolines, hydroxyquinolines (HQs) are the most exploited in medicinal chemistry. Due to their metal chelation properties, not present in the other monohydroxyquinolines, 8-HQ derivatives are exploited as promising therapeutic agents for the treatment of pathologies resulting from metal-ions imbalance and oxidative stress as well as common issues, *e.g.*, in neurodegenerative disorders. Most of their biological action is believed to result from their metal chelation properties towards many transition metal cations [4,10–13]. Concerning their therapeutic action, it is interesting to point out that, in general, metal complexes of 8-HQ derivatives are more effective when compared to the free ligands, being their chelating activity directly involved on their therapeutic effect [14]. This is the case of, for example, clioquinol (5-chloro-7-iodo-quinolin-8-ol, CQ), whose chelation ability towards specific ions like, *e.g.*, Zn^{2+} or Cu^{2+}, is used to activate cell signaling processes involved in neuroprotective cascades, enabling CQ and 8-HQ to inhibit, in Alzheimer's disease, toxic metal-induced Aβ aggregation, with satisfactory anti-neurodegenerative effects [4,15,16]. Another

* Corresponding author.
** Corresponding author at: Centro de Ciências e Tecnologias Nucleares, Instituto Superior Técnico, Universidade de Lisboa, Estrada Nacional 10 (km 139.7), 2695-066 Bobadela LRS, Portugal.
E-mail addresses: sgarlata@unict.it (C. Sgarlata), dmilea@unime.it (D. Milea), sofia.gama@ctn.tecnico.ulisboa.pt (S. Gama).

https://doi.org/10.1016/j.molliq.2024.126671
Received 23 July 2024; Received in revised form 5 November 2024; Accepted 1 December 2024
Available online 5 December 2024

interesting example is the use of Fe^{3+}/8-HQ complexes as cytostatic drugs [4,17]. These results are also consistent with studies on 8-HQA (8-hydroxyquinoline-2-carboxylic acid), which reported its essential role in the regulation of bacterial diversity and abundance in the larvae of *Spodoptera littoralis* midgut, mainly due to its action as a metallophore [18,19].

Following our recent study [20] on the dependence on temperature of the acid-base properties of 8-HQA and its precursors (such as 8-HQ), this work reports results of a detailed investigation of the chemical speciation of 2-HQ, 4-HQ and 6-HQ (denoted in this work as x-HQs, together with 8-HQ), to evaluate the impact of the hydroxyl group position on the acid-base properties of the ligands. For a better interpretation of the biological activity of complex organic molecules, this knowledge is fundamental. As such, in this work, we determined the protonation constants of x-HQs by UV–Vis spectrophotometry and isothermal titration calorimetry (ITC) at $T = 298.15$ K, and by potentiometric titrations (ISE-H^+ glass electrode) at various temperatures ($288.15 \leq T/K \leq 318.15$). All measurements were performed in $KCl_{(aq)}$ at $I = 0.2$ mol·dm^{-3}. The protonation thermodynamic parameters of the mentioned x-HQs were also obtained. For this purpose, based on our previous experience [20], results obtained employing the van't Hoff equation and ITC were critically analyzed and compared. Overall, the analysis of the results from all the different techniques allowed us to fully characterize the thermodynamic profile and the chemical speciation of the studied x-HQs and, most importantly, to analyze the effect of the hydroxyl group position on the acid-base properties of x-HQs.

2. Materials and methods

2.1. Chemicals

Aqueous solutions of quinolin-2-ol (2-hydroxyquinoline, 2-HQ), quinolin-4-ol (4-hydroxyquinoline, 4-HQ), quinolin-6-ol (6-hydroxyquinoline, 6-HQ), quinolin-8-ol (8-hydroxyquinoline, 8-HQ), as well as KCl were prepared weighing the pure compounds. The latter solution was prepared weighing the pure salt after drying for not less than 2 h at $T = 383$ K. HCl and KOH ampoules were purchased from POCH S.A. (Gliwice, Poland), diluted and standardized against Tris (tris(hydroxymethyl)aminomethane) and potassium hydrogen phthalate, respectively, also dried for not less than 2 h at $T = 353$ K in the former and $T = 383$ K in the latter case. All other reagents were purchased from Sigma-Aldrich Europe. All chemicals were of analytical grade purity. Solutions were prepared in grade A glassware and in ultrapure water ($R = 18$ MΩ cm^{-1}).

2.2. ISE-H^+ potentiometry

Potentiometric titrations were performed at the desired temperatures ($288.15 \leq T/K \leq 318.15$) using a combined ISE-$H^+$ glass electrode (model Orion 8102 ROSS Ultra) on a potentiometric titrator (model Orion Star T910), all from Thermo Scientific, USA. The accuracy was ± 0.002 cm^3 and ± 0.2 mV for titrant volume and e.m.f. readings, respectively. All titrations were performed in glass cells under controlled temperature (by water circulation), magnetic stirring, and $Ar_{(g)}$ bubbling to avoid $CO_{2(g)}$ and $O_{2(g)}$ in solution. Several 25 cm^3 solutions were titrated up to pH ~ 11–12 with standardized $KOH_{(aq)}$. Titrant solutions were prepared with different concentrations of x-HQs ($2 \leq c_L$/mmol·dm$^{-3} \leq 6$), $HCl_{(aq)}$ ($8 \leq c_H$/mmol·dm$^{-3} \leq 10$) and KCl ($I = 0.2$ mol·dm^{-3}). For each titration, 100–120 data points were recorded. Each measurement was preceded by electrode calibration (in free H^+ concentration) by alkalimetric ($KOH_{(aq)}$) titrations of $HCl_{(aq)}$ at the same temperature, ionic medium, and ionic strength conditions of the measurements.

2.3. UV–Vis spectrophotometry

UV–Vis spectrophotometric titrations were performed using an Evolution One Plus (Thermo Scientific, USA) UV–Vis spectrophotometer bearing an optical fiber in the sample cell. Spectra were recorded in the wavelength range $200 \leq \lambda$/nm ≤ 800. All measurements were carried out using the same procedure as for potentiometric titrations, *i.e.,* under $Ar_{(g)}$, in $KCl_{(aq)}$ ($I = 0.2$ mol·dm^{-3}), and at $T = 298.15 \pm 0.1$ K, using standardized $KOH_{(aq)}$ as titrant. Each sample was prepared directly in the thermostatted cell, with the total sample volume of 30 cm^3. Equilibrium conditions between each addition of titrant (up to pH ~ 11–12) were controlled with the same potentiometric system previously described.

2.4. Isothermal titration calorimetry (ITC)

Calorimetric titrations were performed at $I = 0.2$ mol·dm^{-3} ($KCl_{(aq)}$) and $T = 298.15$ K, with a Nano-ITC calorimeter from TA Instruments, USA, equipped with an active cell ($V = 0.988$ cm^3) operating in the overfilled mode and an injection syringe of 0.250 cm^3 volume. ITC measurements were conducted by titrating aqueous solutions of 6-HQ ($0.20 \leq c_L$/mmol·dm$^{-3} \leq 0.35$), 4-HQ ($0.25 \leq c_L$/mmol·dm$^{-3} \leq 0.30$) or 2-HQ ($0.30 \leq c_L$/mmol·dm$^{-3} \leq 1.00$), with HNO_3 ($1.80 \leq c_H$/mmol·dm$^{-3} \leq 98.0$), as well as by titrating aqueous solutions of 4-HQ ($0.25 \leq c_L$/mmol·dm$^{-3} \leq 0.30$) or 2-HQ ($0.50 \leq c_L$/mmol·dm$^{-3} \leq 0.6$) with KOH ($15.0 \leq c_{OH}$/mmol·dm$^{-3} \leq 50.0$). HNO_3 was used instead of HCl to avoid the corrosiveness of the latter on stainless steel that is typically used in injection syringes [21]. Titrant (in syringe) and titrate (in cell) solutions were prepared at the desired ionic strength.

Different pH windows, at $1.7 \leq$ pH ≤ 11.8, were monitored to optimize the expected species formation. Typically, three titrations runs were performed for each pH window to record a proper number of data points for a satisfactory curve fitting. The injection time intervals were selected to ensure equilibrium conditions before every addition. Solutions in sample cell were stirred (250 rpm) during titrations. Ultrapure water was used to fill the reference cell. Heats of dilution were obtained separately through proper "blank" experiments performed by titrating either $HNO_{3(aq)}$ or $KOH_{(aq)}$ (in 0.2 mol·dm^{-3} $KCl_{(aq)}$) into $KCl_{(aq)}$ solutions.

All solutions were degassed (under vacuum) and stirred for not less than 15 min before each titration. The instrument was chemically calibrated by a HCl/TRIS test reaction according usual procedures [22], and checked through an electrical calibration. The gross heat evolved/absorbed in the reaction was obtained by integration of the power curve (using the NanoAnalyze software from TA Instruments, USA).

2.5. Calculations

The BSTAC software [23] was used to refine the protonation constants of x-HQs and all parameters of the potentiometric titrations (standard potential (E^0), ionic product of water (pK_w) and the acidic junction coefficient (j_a)). To model the dependence on T of the protonation constants, conversions to the molal scale (mol kg^{-1} (H_2O)) were performed from molar (mol·dm^{-3}) values using the appropriate densities [24].

UV–Vis spectrophotometric data were analyzed by HypSpec2014 software from the Hyperquad suite [25], obtaining both the molar absorbance spectra of the absorbing species and the protonation constants of x-HQs. The program may work using either pH for each point or total proton concentration (c_H) as input. Both modes were adopted during data analysis, yielding the same results.

The reaction net heats (obtained by subtracting the heat absorbed/evolved in the blank experiments) were analyzed by HypCal [26]. This software allows the determination of both protonation constants and enthalpy changes through a minimization procedure based on the non-linear least-squares method.

The speciation diagrams were drawn by means of the PyES program [27].

Protonation constants and other thermodynamic parameters are expressed as stepwise equilibria:

$$H^{+} + H_{i-1}L^{(i-2)} = H_iL^{(i-1)} \log K_i \quad (1)$$

where L stands for fully deprotonated ligands.

Further details on the data analysis are given in ref. [20].

3. Results and discussion

3.1. Protonation constants at $T = 298.15$ K

Despite the availability of new analytical instrumentation and methodologies for chemical speciation investigations, its accurate assessment is still challenging, in particular for complex systems. Though potentiometry remains the elective technique for solution equilibrium studies, a multitechnique approach is always desirable to get further information on the systems under study. Furthermore, each technique provides complementary information, and only when exploiting together a comprehensive definition of the studied systems can be achieved [28]. As such, in this work, UV–Vis spectrophotometric experiments were also performed together with ISE-H^+ potentiometric titrations, enabling the determination of the molar absorbance spectra of x-HQs species, as well as ITC experiments, which also provided the protonation enthalpy and entropy changes. The protonation constants determined by these techniques are shown in Table 1 at $T = 298.15$ K.

The protonation constants of 8-HQ were already determined by potentiometry together with the corresponding thermodynamic parameters (by ITC) [20], while they have been further confirmed in this work by UV–Vis spectrophotometry. As observed, all the obtained results are in excellent accordance.

Fig. 1a presents the experimental absorption spectra of a 6-HQ solution at different pH values, while Fig. 1b shows the calculated molar absorptivity spectra of each species (analogues Figures for other studied ligands are in Supplementary Material, Figures S1-S3).

UV–Vis spectrophotometry was particularly advantageous in case of 2-HQ, as high pH values (pH ~ 12) had to be achieved to determine its log K values. In such conditions, glass electrodes suffer alkaline errors, and, therefore, stability constants obtained may be unreliable if electrode calibrations are not properly performed. Reversely, as already stated in the experimental section, UV–Vis spectra were analyzed by HypSpec2014 [25] considering both pH readings and total proton concentration. In the latter case, results are, of course, not influenced by the electrode errors. Results in Table 1 show that values obtained by potentiometry are in excellent accordance with those by UV–Vis spectrophotometry (and ITC), confirming the accuracy of the potentiometric measurements performed, including electrode calibrations.

ITC measurements are mainly used to determine the enthalpy changes of a chemical reaction. However, stability constants can be simultaneously determined in some cases. Unlike potentiometry and UV–Vis spectrophotometry, ITC does not permit the reliable study of wide pH ranges, as the heat involved in each protonation step can vary considerably. Furthermore, multiple species might simultaneously form in solution, making the deconvolution of the recorded heat quite challenging. Therefore, the study of protonation equilibria using calorimetry requires an *ad hoc* experimental design. Consequently, the pH windows for ITC titrations were properly chosen to maximize species formation according to the speciation diagrams computed by using the outcome from the other techniques. Typical calorimetric titrations for the 4-HQ ligand obtained at suitable pH ranges are shown in Fig. 2, whereas titrations for 6-HQ and 2-HQ are shown in Figures S4 and S5.

Calorimetric titrations intended to explore a more acidic pH region (up to 1.7) did not provide evidence for the protonation equilibria: as shown in Figure S6*a*, the overlap between titration and blank experiments (along with the negligible recorded net heats) indicates that no detectable reaction occurred in the cell upon titration. Furthermore, investigating lower pH values would cause large uncertainty due to the very acidic conditions and high risk for the instrument's performance. Calorimetric data collected for each x-HQ at different pH windows were analyzed by HypCal [26], which can simultaneously refine data from multiple titrations.

Despite the wide number published studies on HQ derivatives, information is lacking concerning the acid-base properties of the studied x-HQs, especially at temperatures other than $T = 298.15$ K, which can be relevant, *e.g.*, for chemical speciation investigations in biological fluids. The only possible comparison with literature data can be achieved for 8-HQ findings from our previous work [21]. There, the sequence for its (de)protonation was also established and, comparing the protonation constants of 8-HQ with those of the ligands investigated in this work, it is possible to confirm it also for other x-HQs studied in this work, *i.e.*, the phenolate is the first group to be protonated with the quinolinic nitrogen coming next. However, in case of 2-HQ we determined only one log K value, since the protonation of its quinolinic nitrogen takes place at very acidic pH.

3.2. Protonation constants at various temperatures and thermodynamic parameters

The experimental protonation constants of 2-HQ, 4-HQ, 6-HQ, and 8-HQ, determined at different temperatures by potentiometry, are reported in Table 2.

The influence of temperature on the acid-base properties of x-HQs is illustrated by the speciation diagrams of 4-HQ at different temperatures, presented in Fig. 3 (the diagrams for 2-HQ and 6-HQ are in Figures S7 and S8).

The fully protonated H_2L^+ species is only formed at pH < 4, with similar percentage at all temperatures (with ~ 50 % at pH ~ 2.3). Accordingly, the first deprotonation step, involving quinoline nitrogen, is only slightly temperature-dependent. The monoprotonated HL species is the major species at 2.5 ≤ pH ≤ 10.5, *i.e.*, that of many natural fluids. It is necessary to stress that the second deprotonation step of 4-HQ (*i.e.*, that of the hydroxyl group) is much more influenced by temperature. Namely, a slight shift towards lower pH is noted for the formation of the L^- species (*i.e.*, the fully deprotonated) with increasing temperature: free 4-HQ formation occurs at pH ~ 8 and achieves 50 % at pH ~ 11.4 at $T = 288.15$ K, and pH ~ 10.5 for other temperatures.

Protonation constants at various temperatures reported in Table 2 for all x-HQs may also be exploited for the modeling of their dependence on T through the van't Hoff equation, allowing the estimation of the corresponding protonation enthalpy changes and, thus, the protonation

Table 1
Protonation constants of x-HQs determined by ISE-H^+ potentiometry, UV–Vis spectrophotometry and ITC at $I = 0.2$ mol·dm^{-3} ($KCl_{(aq)}$) and $T = 298.15$ K.

Ligand	Equilibrium	log K_i [a]		
		ISE-H^+	UV–Vis	ITC
2-HQ	$H^+ + L^- \rightleftharpoons HL$	11.73 ± 0.03	11.78 ± 0.01	11.70 ± 0.04
4-HQ	$H^+ + L^- \rightleftharpoons HL$	10.81 ± 0.01	10.81 ± 0.08	10.73 ± 0.04
	$HL + H^+ \rightleftharpoons H_2L^+$	2.341 ± 0.001	2.40 ± 0.08	2.35 ± 0.06
6-HQ	$H^+ + L^- \rightleftharpoons HL$	8.781 ± 0.002	8.805 ± 0.004	8.9 ± 0.4
	$HL + H^+ \rightleftharpoons H_2L^+$	5.159 ± 0.003	5.168 ± 0.007	4.7 ± 0.4
8-HQ	$H^+ + L^- \rightleftharpoons HL$	9.639 [b]	9.789 ± 0.004	– [c]
	$HL + H^+ \rightleftharpoons H_2L^+$	4.991 [b]	4.823 ± 0.001	– [c]

[a] ±standard deviation.
[b] From ref. [20].
[c] Not determined.

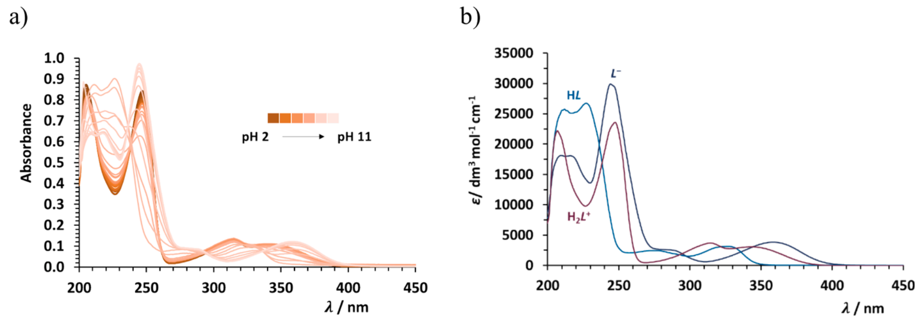

Fig. 1. a) Absorption spectra of 6-HQ recorded at $2 \leq pH \leq 11$ ($c_L = 3 \times 10^{-5}$ mol·dm^{-3}); b) calculated molar absorbance spectra of the formed species.

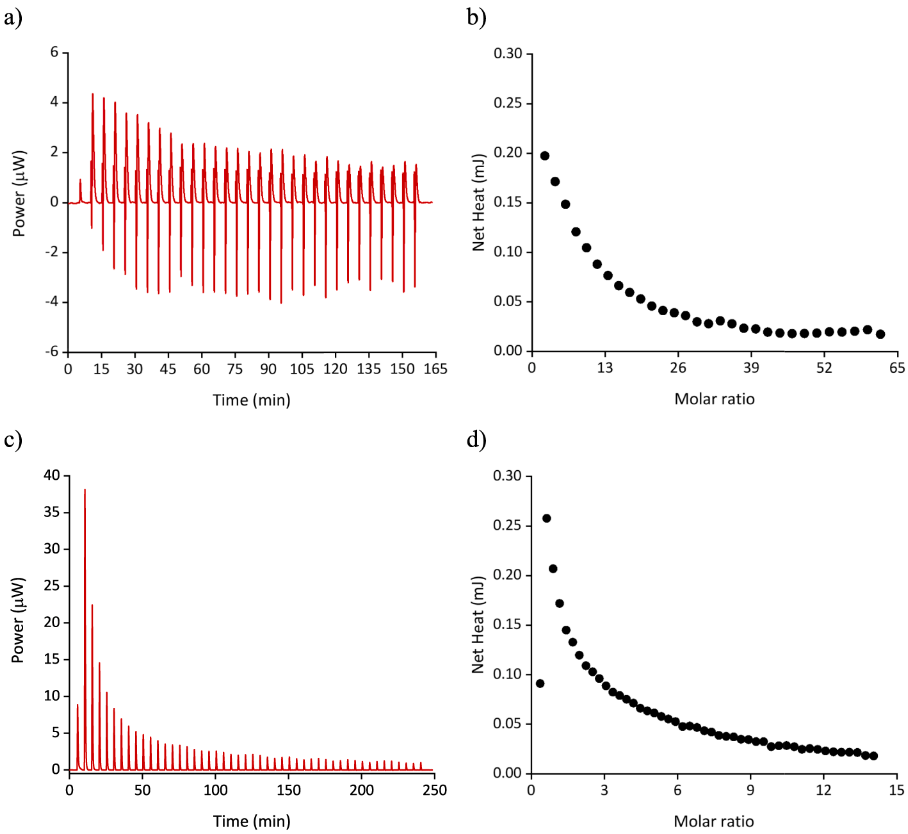

Fig. 2. Typical ITC titration of a) 4-HQ (0.27 mmol·dm^{-3}) by HNO_3 (60.0 mmol·dm^{-3}) in the range $4.2 \geq pH \geq 1.9$, b) integrated heat data; and c) 4-HQ (0.30 mmol·dm^{-3}) by KOH (15.0 mmol·dm^{-3}) in the range $6.9 \leq pH \leq 11.2$, d) integrated heat data.

entropies. More details are given, *e.g.*, in ref. [20]. An example of van't Hoff plot is reported in Fig. 4 for the protonation constants of 6-HQ, while those of 2-HQ and 4-HQ are given as supplementary information (Figures S9 and S10, respectively).

The complete set of thermodynamic parameters calculated by this procedure is reported in Table 3.

Van't Hoff plots and the calculations of enthalpy changes by his equation are usually carried out when their experimental determination is not accessible and, mainly, to verify the linearity of the temperature dependence of these constants (*i.e.*, the enthalpy changes constancy over the investigated temperature range). However, as discussed in detail elsewhere [20,28], direct ITC measurements are preferable, when possible.

As such, calorimetric experiments allowed us to further determine the protonation enthalpy changes of the hydroxylate and nitrogen moieties by direct measurement of the heat released/absorbed during the process. This enabled a comprehensive thermodynamic characterization that is crucial for determining the driving forces of the protonation equilibria and their dependence on the ligand structure. Indeed, the thermodynamic profile includes factors and features having often different entropic and enthalpic terms (*e.g.*, the interaction between the functional groups on the ligands and protons, structural reorganization, desolvation, etc.). Thus, dissecting the ΔG^0 value into its components allows for the analysis of insights on the protonation equilibria not displayed by the log K value alone [29,30]. Thermodynamic protonation parameters of x-HQs ligands obtained by ITC experiments are shown in Table 4.

Noteworthy, though the differences between direct ITC measurements and the van't Hoff approach [20], and considering the associated uncertainties too, values reported in Tables 3 and 4 are in excellent agreement for all the investigated ligands.

All the protonation steps of x-HQs occur through a spontaneous process, as observable from the negative Gibbs free energies. These values strongly depend on the hydroxyl group's position on the

Table 2
Experimental protonation constants of 2-HQ, 4-HQ, 6-HQ, and 8-HQ at different temperatures, determined by ISE-H^+ potentiometry.

Ligand	Equilibrium	log K_i [a]		
		288.15 K	310.15 K	318.15 K
2-HQ	$H^+ + L^- \rightleftharpoons HL$	12.09 ± 0.02	11.405 ± 0.009	11.28 ± 0.02
4-HQ	$H^+ + L^- \rightleftharpoons HL$	11.340 ± 0.004	10.713 ± 0.002	10.528 ± 0.001
	$HL + H^+ \rightleftharpoons H_2L^+$	2.364 ± 0.003	2.341 ± 0.004	2.279 ± 0.001
6-HQ	$H^+ + L^- \rightleftharpoons HL$	8.923 ± 0.001	8.673 ± 0.002	8.608 ± 0.002
	$HL + H^+ \rightleftharpoons H_2L^+$	5.319 ± 0.002	5.042 ± 0.003	4.940 ± 0.004
8-HQ[b]	$H^+ + L^- \rightleftharpoons HL$	9.808	9.47	9.385
	$HL + H^+ \rightleftharpoons H_2L^+$	5.16	4.789	4.679

[a] ±standard deviation.
[b] From ref. [20].

Table 3
Protonation thermodynamic parameters (ΔG^0, ΔH^0, $T\Delta S^0$) of x-HQs calculated by the van't Hoff equation at $T = 298.15$ K.

Ligand	Equilibrium	ΔG_i^0 [a,b]	ΔH_i^0 [a,c]	$T\Delta S_i^0$ [a,d]
2-HQ	$H^+ + L^- \rightleftharpoons HL$	−66.96	−47.9	19
4-HQ	$H^+ + L^- \rightleftharpoons HL$	−61.71	−43.7	18
	$HL + H^+ \rightleftharpoons H_2L^+$	−13.36	−3.9	9
6-HQ	$H^+ + L^- \rightleftharpoons HL$	−50.13	−18.2	32
	$HL + H^+ \rightleftharpoons H_2L^+$	−29.45	−21.5	8
8-HQ[e]	$H^+ + L^- \rightleftharpoons HL$	−55.03	−24.9	30
	$HL + H^+ \rightleftharpoons H_2L^+$	−28.49	−28.4	0

[a] in kJ mol^{-1}.
[b] ±0.01 – 0.05 kJ mol^{-1}.
[c] ± 0.1 – 0.5 kJ mol^{-1}.
[d] ± 1 – 2 kJ mol^{-1}.
[e] From ref. [20].

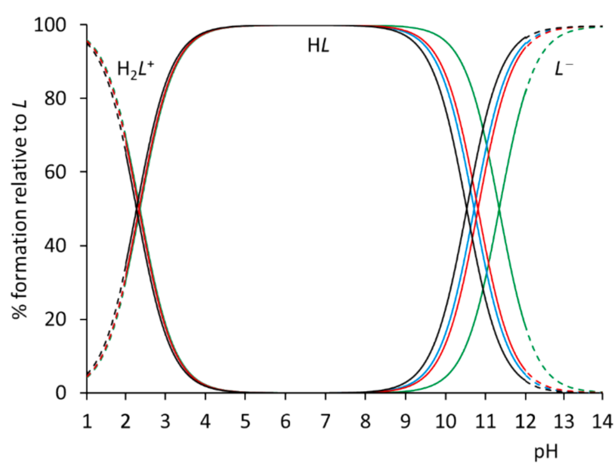

Fig. 3. Distribution diagram of 4-HQ species *vs.* pH at different temperatures: T = 288.15 K (green), 298.15 K (red), 310.15 K (blue), 318.15 K (black). Experimental conditions: $c_L = 10^{-3}$ mol·dm^{-3}. The dashed lines at pH < 2.0 and pH > 12.0 refer to pH ranges not experimentally accessed.

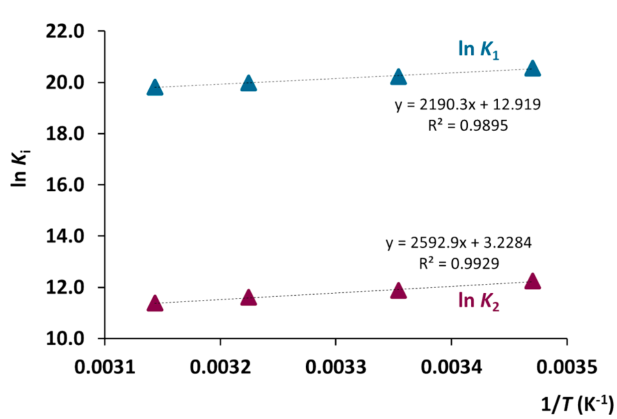

Fig. 4. Van't Hoff plots of ln K_i *vs.* $1/T$ for 6-HQ.

Table 4
Thermodynamic protonation parameters (ΔG^0, ΔH^0, $T\Delta S^0$) of x-HQs determined by ITC at $T = 298.15$ K.

Ligand	Equilibrium	ΔG_i^0 [a,b]	ΔH_i^0 [a,c]	$T\Delta S_i^0$ [a,d]
2-HQ	$H^+ + L^- \rightleftharpoons HL$	−66.8	−47.48	19.3
4-HQ	$H^+ + L^- \rightleftharpoons HL$	−61.3	−41.18	20.1
	$HL + H^+ \rightleftharpoons H_2L^+$	−13.4	−8.83	4.6
6-HQ	$H^+ + L^- \rightleftharpoons HL$	−50.8	−22.67	28.1
	$HL + H^+ \rightleftharpoons H_2L^+$	−26.8	−28.99	−2.2
8-HQ[e]	$H^+ + L^- \rightleftharpoons HL$	−55.03	−24.9	30
	$HL + H^+ \rightleftharpoons H_2L^+$	−28.49	−28.4	0

[a] in kJ mol^{-1}.
[b] ± 0.1 – 2.1 kJ mol^{-1}.
[c] ± 0.01 – 0.05 kJ mol^{-1}.
[d] ± 0.1 – 2.1 kJ mol^{-1}.
[e] From ref. [20].

molecule's aromatic rings, and its proximity to the quinoline nitrogen. The ΔG^0 values for the protonation of the hydroxylate follow the order 2-HQ > 4-HQ > 8-HQ > 6-HQ. The proximity of –OH to the nitrogen of the aromatic ring of x-HQs influences the spontaneity of the protonation process, which decreases as the distance between the two moieties increases. An analogous trend is observable for the protonation of the quinoline nitrogen: in this case, the ΔG^0 increases in the order 4-HQ < 6-HQ ≤ 8-HQ. The protonation of the hydroxyl group of all ligands exhibits favorable enthalpic and entropic contributions. For 4-HQ and 2-HQ, the first protonation event is enthalpy driven, while the entropic gain, likely ascribable to desolvation, drives the protonation of hydroxylate in 6-HQ. Interestingly, the enthalpic gain for the first protonation decreases with the increase of the distance of the hydroxylate from the aromatic nitrogen, according to the sequence 2-HQ > 4-HQ > 8-HQ > 6-HQ. The same trend is observed for the hydroxylate protonation process, whose acidity decreases as the proximity between the two groups decreases. The enthalpy changes determined for the first protonation equilibrium of 4-HQ and 2-HQ are pretty comparable with each other, while they are, on average, about 20 kJ mol^{-1} larger than those of 6-HQ and 8-HQ. The protonation of the nitrogen in the aromatic ring is enthalpically favored and driven for both the 4-HQ and 6-HQ ligands with a small (favorable and unfavorable, respectively) entropy contribution. The high acidity of the quinoline nitrogen of 2-HQ hampered the determination of the parameters for its second protonation reaction. Again, as the distance between the hydroxyl group and the quinoline nitrogen increases, the entropic gain decreases and becomes even more unfavorable in the case of 6-HQ. All these aspects can be better visualized in Fig. 5.

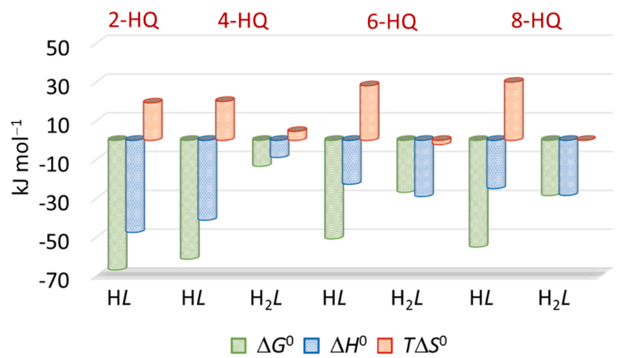

Fig. 5. Thermodynamic protonation parameters of x-HQs at $T = 298.15$ K.

3.3. *Effect of hydroxyl group position on thermodynamic protonation parameters*

The remarkable differences among the protonation constants of the four regioisomeric x-HQs derivatives can be explained by taking into account the tautomeric equilibria between hydroxyquinoline and oxoquinoline (quinolone) forms experienced by 2-HQ and 4-HQ (Fig. 6) [31]. Tautomerization results in a variation of the chemical and physical properties of these compounds, which directly reflects on their proclivity to protonation.

The quinolone tautomer of 2-HQ, in particular, is a very stable cyclic amide, and this explains the evidence that 2-HQ shows the highest log K_1 (relative to the protonation of L^- to give HL) and that log K_2 (*i.e.*, HL to H_2L^+) could not be determined (Table 1), since an amide nitrogen atom is less prone to protonation than a pyridine-type one. Analogously, in the 4-HQ oxoquinoline tautomer, the C═O and NH groups are arranged in a stable pyridin-4-one system, resulting again in a high log K_1 (HL) and very low log K_2 (H_2L^+). 6-HQ and 8-HQ do not experience similar equilibria (their tautomeric forms are non-Kekuléan [32]), and therefore they mainly exist in their hydroxyquinoline form. The log K_1 (HL) and log K_2 (H_2L^+) for 6-HQ do not significantly differ from those of pyridine and phenol, indicating that there is only a modest electronic interaction between the two functional groups. However, as for 8-HQ, a slight increase in log K_1 (HL) along with a decrease in the log K_2 (H_2L^+) is observed, probably due to an intramolecular O─H⋯N hydrogen bond (Fig. 6c) that makes, at the same time, the hydrogen atom harder to extract and the ring nitrogen less basic.

Overall, for the above reasons, the thermodynamic profile of the investigated ligands appears to be severely affected by their structural features and, in particular, by the position of the hydroxyl moiety on the two different aromatic rings of the quinoline scaffold. Indeed, the thermodynamic fingerprint for the protonation of 4-HQ and 2-HQ, which bear the –OH group in the same aromatic ring containing the nitrogen, shows similar features. Conversely, for both 6-HQ and 8-HQ, the protonation of the phenolate is entropy driven along with a favorable enthalpic contribution, which is instead the only term favorably contributing to Gibbs free energy in the protonation of the nitrogen moiety.

4. Conclusions

In this work, an investigation of the chemical speciation of x-HQs is reported, aiming at evaluating the effect of the hydroxyl group position on the acid-base properties of the studied ligands. Using a multi-technique approach, we determined the pronation constants of x-HQs as well as other thermodynamic protonation parameters, namely protonation enthalpy and entropy changes. Results obtained by different techniques for the protonation constants are in excellent agreement. Phenolate is the first group undergoing protonation, followed by quinolinic nitrogen. The tautomeric equilibria between hydroxyquinoline and oxoquinoline (quinolone) forms present in 2-HQ and 4-HQ leads to a considerable increase of the acidity of proton bound to the quinolinic nitrogen, resulting in very low values of log K (*e.g.*, log $K < 2$ for 2-HQ). The protonation of the hydroxyl group of all ligands exhibits favorable enthalpic and entropic contributions, while that of the quinolinic nitrogen is generally enthalpically driven.

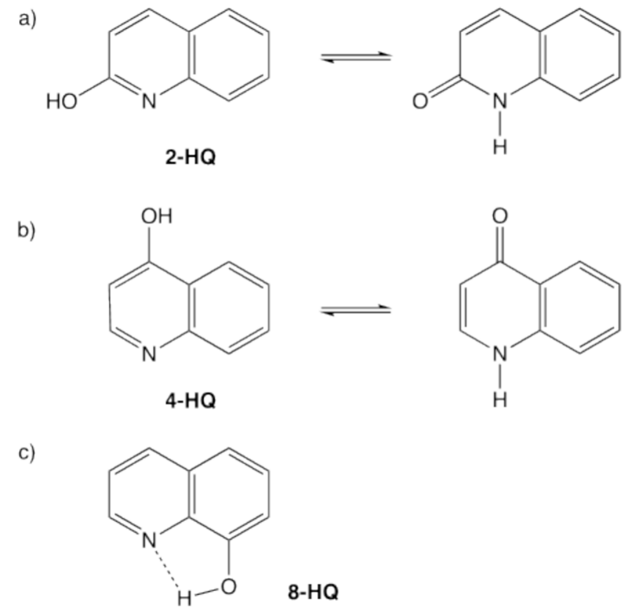

Fig. 6. Tautomeric equilibria for a) 2-HQ and b) 4-HQ; c) intramolecular hydrogen bond in 8-HQ.

Summarizing, we can affirm that the hydroxyl group position in the quinoline structure of x-HQs deeply affects both the stability and the driving forces leading the protonation/deprotonation processes of both the quinolinic nitrogen and the hydroxyl groups.

CRediT authorship contribution statement

Anna Baryłka: Writing – original draft, Investigation. **Giuseppina D.G. Santonoceta:** Writing – original draft, Investigation. **Giuseppe Gattuso:** Writing – review & editing, Formal analysis, Data curation. **Beata Godlewska-Żyłkiewicz:** Writing – review & editing, Resources, Project administration, Funding acquisition. **Carmelo Sgarlata:** Writing – review & editing, Validation, Resources, Methodology, Formal analysis, Data curation. **Demetrio Milea:** Writing – review & editing, Validation, Supervision, Resources, Project administration, Methodology, Funding acquisition, Formal analysis, Data curation, Conceptualization. **Sofia Gama:** Writing – review & editing, Validation, Supervision, Resources, Project administration, Methodology, Funding acquisition, Formal analysis, Data curation, Conceptualization.

Declaration of competing interest

The authors declare that they have no known competing financial interests or personal relationships that could have appeared to influence the work reported in this paper.

Acknowledgments

The authors would like to acknowledge financial support from the National Science Centre (NCN), Poland, under the research project number 2020/39/B/ST4/03060, and the financial support under the National Recovery and Resilience Plan (NRRP), Mission 4, Component 2, Investment 1.1, Call for tender No. 1409 published on 14.9.2022 by the Italian Ministry of University and Research (MUR), funded by the

European Union – NextGenerationEU– Project Title Efficient Sequestration of Metal Ions from Aqueous Systems for Green and Sustainable Applications - AquaGreen – CUP J53D23014430001- Grant Assignment Decree No. 1409 adopted on 14/09/2022 by the Italian Ministry of Ministry of University and Research (MUR).

Appendix A. Supplementary data

Supplementary data to this article can be found online at https://doi.org/10.1016/j.molliq.2024.126671.

Data availability

Data will be made available on request.

References

[1] C. Sgarlata, G. Arena, R.P. Bonomo, A. Giuffrida, G. Tabbi, Simple and mixed complexes of copper(II) with 8-hydroxyquinoline derivatives and amino acids: Characterization in solution and potential biological implications, J. Inorg. Biochem. 180 (2018) 89–100.

[2] S.H. Chan, C.H. Chui, S.W. Chan, S.H. Kok, D. Chan, M.Y. Tsoi, P.H. Leung, A. K. Lam, A.S. Chan, K.H. Lam, J.C. Tang, Synthesis of 8-hydroxyquinoline derivatives as novel antitumor agents, ACS Med. Chem. Lett. 4 (2013) 170–174.

[3] M. Kubanik, H. Holtkamp, T. Söhnel, S.M.F. Jamieson, C.G. Hartinger, Impact of the Halogen Substitution Pattern on the Biological Activity of Organoruthenium 8-Hydroxyquinoline Anticancer Agents, Organometallics 34 (2015) 5658–5668.

[4] V. Prachayasittikul, S. Prachayasittikul, S. Ruchirawat, V. Prachayasittikul, 8-Hydroxyquinolines: a review of their metal chelating properties and medicinal applications, Drug Des. Devel. Ther. 7 (2013) 1157–1178.

[5] P. Yadav, K. Shah, Quinolines, a perpetual, multipurpose scaffold in medicinal chemistry, Bioorg. Chem. 109 (2021) 104639.

[6] A. Weyesa, E. Mulugeta, Recent advances in the synthesis of biologically and pharmaceutically active quinoline and its analogues: a review, RSC Adv. 10 (2020) 20784–20793.

[7] S. Madapa, Z. Tusi, D. Sridhar, A. Kumar, M.I. Siddiqi, K. Srivastava, A. Rizvi, R. Tripathi, S.K. Puri, G.B. Shiva Keshava, P.K. Shukla, S. Batra, Search for new pharmacophores for antimalarial activity. Part I: synthesis and antimalarial activity of new 2-methyl-6-ureido-4-quinolinamides, Bioorg. Med. Chem. 17 (2009) 203–221.

[8] A.M. Gilbert, M.G. Bursavich, S. Lombardi, K.E. Georgiadis, E. Reifenberg, C. R. Flannery, E.A. Morris, N-((8-hydroxy-5-substituted-quinolin-7-yl)(phenyl) methyl)-2-phenyloxy/amino-acetamide inhibitors of ADAMTS-5 (Aggrecanase-2), Bioorg. Med. Chem. Lett. 18 (2008) 6454–6457.

[9] R. Musiol, An overview of quinoline as a privileged scaffold in cancer drug discovery, Expert Opin. Drug Discov. 12 (2017) 583–597.

[10] A. Budimir, Metal ions, Alzheimer's disease and chelation therapy, Acta Pharm. 61 (2011) 1–14.

[11] R.R. Crichton, D.T. Dexter, R.J. Ward, Metal based neurodegenerative diseases—From molecular mechanisms to therapeutic strategies, Coord. Chem. Rev. 252 (2008) 1189–1199.

[12] L. Li, H. Wu, J. Wang, Z. Ji, T. Fang, H. Lu, L. Yan, F. Shen, D. Zhang, Y. Jiang, T. Ni, Discovery of Novel 8-Hydroxyquinoline Derivatives with Potent In Vitro and In Vivo Antifungal Activity, J. Med. Chem. 66 (2023) 16364–16376.

[13] C. Bissani Gasparin, D.A. Pilger, 8-Hydroxyquinoline, Derivatives and Metal-Complexes: A Review of Antileukemia Activities, ChemistrySelect 8 (2023) e202204219.

[14] A. Barilli, C. Atzeri, I. Bassanetti, F. Ingoglia, V. Dall'Asta, O. Bussolati, M. Maffini, C. Mucchino, L. Marchio, Oxidative stress induced by copper and iron complexes with 8-hydroxyquinoline derivatives causes paraptotic death of HeLa cancer cells, Mol. Pharm. 11 (2014) 1151–1163.

[15] X. Yang, P. Cai, Q. Liu, J. Wu, Y. Yin, X. Wang, L. Kong, Novel 8-hydroxyquinoline derivatives targeting beta-amyloid aggregation, metal chelation and oxidative stress against Alzheimer's disease, Bioorg. Med. Chem. 26 (2018) 3191–3201.

[16] R. Gupta, V. Luxami, K. Paul, Insights of 8-hydroxyquinolines: A novel target in medicinal chemistry, Bioorg. Chem. 108 (2021) 104633.

[17] Y.N. Song, H. Xu, W.M. Chen, P. Zhan, X.Y. Liu, 8-Hydroxyquinoline: a privileged structure with a broad-ranging pharmacological potential, Med. Chem. Comm. 6 (2015) 61–74.

[18] S. Gama, M. Frontauria, N. Ueberschaar, G. Brancato, D. Milea, S. Sammartano, W. Plass, Thermodynamic study on 8-hydroxyquinoline-2-carboxylic acid as a chelating agent for iron found in the gut of Noctuid larvae, New J. Chem. 42 (2018) 8062–8073.

[19] K. Arena, G. Brancato, F. Cacciola, F. Crea, S. Cataldo, C. De Stefano, S. Gama, G. Lando, D. Milea, L. Mondello, A. Pettignano, W. Plass, S. Sammartano, 8-Hydroxyquinoline-2-Carboxylic Acid as Possible Molybdophore: A Multi-Technique Approach to Define Its Chemical Speciation, Coordination and Sequestering Ability in Aqueous Solution, Biomolecules 10 (2020) 930.

[20] A. Baryłka, A. Bagińska-Krakówka, L. Zuccarello, F. Mancuso, G. Gattuso, G. Lando, C. Sgarlata, C. De Stefano, B. Godlewska-Żyłkiewicz, D. Milea, S. Gama, Protonation equilibria of the tryptophan metabolite 8-hydroxyquinoline-2-carboxylic acid (8-HQA) and its precursors: A potentiometric and calorimetric comparative study, Thermochim. Acta 730 (2023) 179615.

[21] Ž. Medoš, M. Bešter-Rogač, E. Leontidis, J. Tellinghuisen, Calibrating ITC instruments: Problems with weak base neutralization, Anal. Biochem. 694 (2024) 115602.

[22] C. Sgarlata, V. Zito, G. Arena, Conditions for calibration of an isothermal titration calorimeter using chemical reactions, Anal. Bioanal. Chem. 405 (2013) 1085–1094.

[23] C. De Stefano, S. Sammartano, P. Mineo, C. Rigano, Computer Tools for the Speciation of Natural Fluids, in: A. Gianguzza, E. Pelizzetti, S. Sammartano (Eds.), Marine Chemistry - an Environmental Analytical Chemistry Approach, Kluwer Academic Publishers, Amsterdam, 1997, pp. 71–83.

[24] H.S. Harned, B.B. Owen, The physical chemistry of electrolytic solutions Reinhold Pub. Corp, Third edition ed., New York, 1958.

[25] P. Gans, Hyperquad, http://www.hyperquad.co.uk/, Accessed: July 2024.

[26] G. Arena, P. Gans, C. Sgarlata, HypCal, a general-purpose computer program for the determination of standard reaction enthalpy and binding constant values by means of calorimetry, Anal. Bioanal. Chem. 408 (2016) 6413–6422.

[27] L. Castellino, E. Alladio, S. Bertinetti, G. Lando, C. De Stefano, S. Blasco, E. García-España, S. Gama, S. Berto, D. Milea, PyES – An open-source software for the computation of solution and precipitation equilibria, Chemom. Intell. Lab. Syst. 239 (2023) 104860.

[28] A. Baryłka, B. Godlewska-Żyłkiewicz, D. Milea, S. Gama, The accurate assessment of the chemical speciation of complex systems through multi-technique approaches, Pure Appl. Chem. 96 (2024) 597–623.

[29] G. Arena, C. Bretti, G.I. Grasso, G. Lando, S. Sammartano, C. Sgarlata, Thermodynamic study on levulinic acid in NaCl, $(C_2H_5)_4NI$ and mixed $MgCl_2$/NaCl and $CaCl_2$/NaCl aqueous solutions at T = 298.15 K, J. Chem. Thermodyn. 139 (2019) 105870.

[30] C. Bretti, C. De Stefano, P. Cardiano, S. Cataldo, A. Pettignano, G. Arena, C. Sgarlata, G. Ida Grasso, G. Lando, S. Sammartano, Risedronate complexes with Mg^{2+}, Zn^{2+}, Pb^{2+}, and Cu^{2+}: Species thermodynamics and sequestering ability in $NaCl_{(aq)}$ at different ionic strengths and at T298.15 K, J. Mol. Liq. 343 (2021) 117699.

[31] A. Albert, J.N. Phillips, 264. Ionization constants of heterocyclic substances. Part II. Hydroxy-derivatives of nitrogenous six-membered ring-compounds, J. Chem. Soc. (1956) 1294–1304.

[32] G. Karpińska, A.P. Mazurek, J.C. Dobrowolski, Hydroxyquinolines: Constitutional isomers and tautomers, Comput. Theor. Chem. 972 (2011) 48–56.